Complete Scaling Analysis of the Metal–Insulator Transition in Ge:Ga: Effects of Doping-Compensation and Magnetic Field

Kohei M. Itoh[1], Michio Watanabe[2], Youiti Ootuka[3], Eugene E. Haller[4] and Tomi Ohtsuki[5]

[1]*Department of Applied Physics and Physico-Informatics, Keio University, Yokohama 223-8522*
[2]*Macroscopic Quantum Coherence Laboratory, FRS, RIKEN, Saitama 351-0198*
[3]*Tsukuba Research Center for Interdisciplinary Materials Science and Institute of Physics, University of Tsukuba, Ibaraki 305-8571*
[4]*UC Berkeley and Lawrence Berkeley National Laboratory, Berkeley, CA 94720, U.S.A.*
[5]*Department of Physics, Sophia University, Tokyo 102-8544*

We report on the complete scaling analysis of low temperature electron transport properties with and without magnetic field in the critical regime for the metal–insulator transition in two series of homogeneously doped p-type Ge samples: i) nominally uncompensated neutron-transmutation-doped (NTD) ^{70}Ge:Ga samples with the technological compensation ratio $K < 0.001$, and ii) intentionally compensated NTD ^{nat}Ge:Ga,As samples with $K = 0.32$. For the case of the uncompensated series in zero magnetic field, the critical exponents μ, ν, and ζ determined for the electrical conductivity (σ), localization length (ξ), and impurity dielectric susceptibility (χ_{imp}), respectively, change at the very vicinity of the critical Ga concentration ($N \sim N_c$). Namely, the anomalous critical exponents, *e.g.* $\mu \approx 0.5$, change to $\mu \approx 1$ only within the region $0.99N_c < N < 1.01N_c$. On the other hand, the same critical behavior, $\mu \approx 1$, was found for the $K = 0.32$ series in much larger region $0.25N_c < N < 2.4N_c$. This finding suggests that the $\mu \approx 1$ critical behavior observed for the nominally uncompensated series in the extremely narrow region is due to the presence of the self-compensation of acceptors by native defects and/or technologically unavoidable very small amount of doping compensation ($K < 0.001$). Therefore, the width of the concentration that can be fitted with $\mu \approx 1$ around N_c is likely to scale with the degree of compensation (K), and disappears in the limit $K \to 0$, i.e., only the region with the anomalous exponent $\mu \approx 0.5$ remains for the case of $K = 0$. An externally applied magnetic field to nominally uncompensated samples also broadens the width of $\mu \approx 1$ around N_c, but with a mechanism clearly different from that of compensation. The unified description of our experimental results unambiguously establishes the values of the critical exponents μ, ν, and ζ for doped semiconductors with and without compensation and magnetic field.

1. Introduction

The metal–insulator (MI) transition in the presence of both disorder and electron–electron interaction turns out to be one of the most challenging subjects in condensed-matter physics. Despite many decades of theoretical[1–6] and experimental efforts,[7–24] researchers are yet to agree upon an unified description of the phenomena.[25] The doping-induced MI transition in single crystalline semiconductors is the best example of disorder and interaction induced transition that has been studied extensively via measurements of physical quantities such as the electrical conductivity, dielectric constant, and heat capacity. In particular, the critical behavior of the electrical conductivity at zero temperature $\sigma(0)$ has been evaluated as a function of a parameter t that describes the degree of the disorder and interaction;

$$\sigma(0) \propto |t/t_c - 1|^{\mu} \qquad (1)$$

where μ is the conductivity critical exponent and t_c is the critical value of t that separates the insulating and metallic phases. The MI transition in semiconductors has been investigated as a function of the doping concentration (N), externally applied magnetic field (B), and externally applied uniaxial stress (S), i.e., $t \equiv N, B, S$, and $t_c \equiv N_c, B_c, S_c$, respectively, in eq. (1). In this paper we probe the MI transition in nominally uncompensated and intentionally compensated Ge:Ga samples by tuning N and B.

Since the classic experiment of Rosenbaum *et al.* that showed $\mu \approx 0.5$ for stress (S)-tuned Si:P,[8] a wide variety of experiments probing the value of μ has been performed on nominally uncompensated semiconductors as a function of N or S in the absence of the externally applied magnetic field B. The results are truly puzzling as summarized in Table I. One immediately sees in Table I that different values of μ have been reported even for the same system. $\mu \approx 0.5$ is puzzling from a theoretical point of view since it violates Chayes *et al.*'s inequality $\mu \geq 2/3$[26] assuming Wegner's scaling law $\mu = \nu$ for the three dimension[27] where ν is the critical exponent for the localization length ξ and for correlation length ξ'.

Table I. Conductivity critical exponents (μ) reported for a wide variety of nominally uncompensated ($K \approx 0$) semiconductors in the absence of externally applied magnetic field.

Semiconductor system	μ
Si:P	0.5,[8] 1.0,[9] 1.2[10]
Si:As	0.5,[11] 1.0[12]
Si:B	0.65,[13] 1.6[14]
Ge:As	0.5,[15] 1.2[12]
Ge:Sb	0.9[16]
Ge:Ga	0.5,[17,18] 1.2[19]

The following example of the Si:P situation illustrates very well how various research groups have reached different values of μ. Because the MI transition discussed here is considered to be a quantum phase transition that occurs at zero temperature, one has to rely on particular theoretical models to extrapolate information, which represents the zero-temperature states of physical parameters such as electrical conductivity σ, localization length ξ, impurity dielectric susceptability χ_{imp}, etc. Rosenbaum *et al.* have measured the temperature dependence of σ of nominally uncompensated Si:P down to $T = 3 \, \text{mK}$ with finely-tuned uniaxial stress S, and estimated the zero temperature conductivity $\sigma(0)$ for a given S by linear extrapolation of σ to $T = 0 \, \text{K}$ assuming $\sigma \propto T^{1/2}$. They determined $\mu \approx 0.5$ by achieving a good fit for a wide range on the metallic side $(0.7 S_\text{c} < S < S_\text{c})$ of $\sigma(0)$ vs S by eq. (1).[8] More recently, a group from Universität Karlsruhe questioned the relatively wide range of N and S that could be fitted with $\mu \approx 0.5$, and proposed $\mu \approx 1.3$ on N-tuned Si:P by redefining N_c at a value 6% smaller than that of Rosenbaum *et al.*, and by limiting the critical region only to $N_\text{c} < N < 1.07 N_\text{c}$.[10] Rosenbaum *et al.* immediately argued that the $\mu \approx 1.3$ region analyzed by the Karlsruhe group was an artifact due to an inhomogeneous dopant distribution,[28] but the Karlsruhe group responded that only the region scalable with the so-called finite temperature analysis should be considered as the true critical region.[29] The finite temperature scaling takes the form;[5]

$$\sigma(t, T) \propto T^x f(|t/t_\text{c} - 1|/T^y). \quad (2)$$

Here $y = 1/z\nu$ where z is the dynamical scaling exponent. The critical exponent is given by $\mu = x/y$. Equation (2) has two advantages over the conventional analysis involving eq. (1). Firstly, eq. (2) allows one to use values of $\sigma(t, T)$ recorded at finite temperatures, i.e., the conventional extrapolation to $T = 0$ can be avoided. Secondly, eq. (2) allows one to evaluate $\sigma(t, T)$ recorded on the both sides of the transition ($t < t_\text{c}$ and $t_\text{c} < t$), while eq. (1) can be used only on the metallic side.

The Karlsruhe group has shown that their N-tuned data scale according to eq. (2) only in the vicinity of N_c and not for the wide range evaluated by Rosenbaum *et al.* In the same spirit, the Karlsruhe group has further analyzed the data of S-tuned Si:P and obtained $\mu \approx 1$ by limiting the critical region only to the vicinity of S_c.[9] In our view, the situation similar to Si:P applies to all the other systems listed in Table I. Researchers, including ourselves,[19] have obtained $\mu \approx 1$ for nominally uncompensated systems only when they have limited the critical region to a very small range, typically within a few percent of N_c or S_c. It should also be noted that the values of μ reported for intentionally compensated samples were always $\mu \approx 1$ for a wide range of N above N_c; very often up to 50% and more.[30–34] The relation between $\mu \approx 1$ observed only in the vicinity of t_c in nominally uncompensated samples and the similar $\mu \approx 1$ observed for a wide range above t_c in intentionally compensated samples must be clarified.

Moreover, it is important to point out that many of the previous experiments performed on the nominally uncompensated samples were not supposed to be able to analyze such a small region, within a few percent of N_c or S_c,

because a typical spatial fluctuation of the doping concentration within a typical sample size of a few mm could easily be a few percent when it was prepared by the standard melt-doping method.[35] In this regards, Rosenbaum *et al.*'s warning against the analysis of the very vicinity of t_c[28] should be taken very seriously. Doping fluctuations also make it impossible to determine N_c and S_c precisely for the reliable determination of μ. Only a few experimental groups, including ourselves, have recognized this problem and employed a method known as neutron-transmutation-doping (NTD) in order to realize completely homogeneous doping down to the atomic level.[15,17–24,32] The NTD preparation of samples is absolutely crucial for the successful scaling analysis as we will show in this paper.

The present paper reports the experimental studies on the effects of the doping compensation and externally applied magnetic field on the MI transition of doped semiconductors. In order to better illustrate the significance of the present results, we shall summarize important conclusions of our earlier results[17–24] at the beginning of the paper, and proceed to the discussion of the compensation and applied magnetic field.

2. Experiment

2.1 Sample preparation and characterization

A chemically very pure ^{70}Ge crystal of isotopic composition $[^{70}\text{Ge}] = 96.2 \, \text{at.\%}$ and $[^{72}\text{Ge}] = 3.8 \, \text{at.\%}$, and a $^{\text{nat}}\text{Ge}$ crystal with natural isotopic abundance $[^{70}\text{Ge}] = 20.5 \, \text{at.\%}$, $[^{72}\text{Ge}] = 27.4 \, \text{at.\%}$, $[^{73}\text{Ge}] = 7.8 \, \text{at.\%}$, $[^{74}\text{Ge}] = 36.5 \, \text{at.\%}$, and $[^{76}\text{Ge}] = 7.8 \, \text{at.\%}$ were grown using the Czochralski method. The as-grown crystals are free of dislocations, p type with an electrically active net-impurity concentration less than $5 \times 10^{11} \, \text{cm}^{-3}$.

A series of nominally uncompensated samples with the compensation ratio $K < 0.001$ were prepared by the following procedure. The thermal neutron irradiation leading to NTD was performed at the University of Missouri Research Reactor with a thermal to fast neutron ratio of $\sim 30 : 1$. Wafers sliced from the ^{70}Ge crystal become p type due to neutron capture $^{70}\text{Ge} + \text{n} \rightarrow {}^{71}\text{Ge}$ followed by electron capture with a half-life of 11.2 days forming a ^{71}Ga acceptor. The small fraction of ^{72}Ge capturing neutron becomes ^{73}Ge which is stable, i.e., no further acceptors or donors are introduced to the ^{70}Ge crystal. The rapid-thermal annealing after NTD at $650°\text{C}$ for $10 \, \text{s}$ removed most of the irradiation-induced defects from the samples. A short annealing time is important in order to avoid the redistribution and/or clustering of the uniformly dispersed ^{71}Ga acceptors. The concentration of the electrically active radiation defects measured with deep level transient spectrometry (DLTS) after the annealing is less than 0.1% of the Ga concentration,[36] i.e., technological $K < 0.001$. Note here that the so called self-compensation near $N \approx N_\text{c}$ may lead to a larger K.[37] The dimension of most samples used for conductivity measurements was $6 \times 0.9 \times 0.7 \, \text{mm}^3$. Four strips of boron-ion-implanted regions on a $6 \times 0.9 \, \text{mm}^2$ face of each sample were coated with 200 nm Pd and 400 nm Au pads using a sputtering technique. Annealing at $300°\text{C}$ for one hour activated the implanted boron and removed the stress in the metal films. The Ga concentration N in our ^{70}Ge samples after NTD is given precisely by

$$[^{71}\text{Ga}]\,(\text{cm}^{-3}) = 0.1155 \times n\,(\text{cm}^{-2}), \qquad (3)$$

where n is the thermal neutron fluence. Therefore, we have an ability to control $N \equiv [^{71}\text{Ga}]$ with the precision of 0.01%.

A series of intentionally compensated samples has been prepared by NTD of the $^{\text{nat}}$Ge crystal using the same procedure as the one employed for the nominally uncompensated ^{70}Ge samples. Upon thermal neutron irradiation, the five stable isotopes of $^{\text{nat}}$Ge undergo the following nuclear reactions after neutron capture: $^{70}\text{Ge} + \text{n} \rightarrow {}^{71}\text{Ge} \rightarrow {}^{71}\text{Ga}$ acceptor, $^{72}\text{Ge} + \text{n} \rightarrow {}^{73}\text{Ge}$, $^{73}\text{Ge} + \text{n} \rightarrow {}^{74}\text{Ge}$, $^{74}\text{Ge} + \text{n} \rightarrow {}^{75}\text{Ge} \rightarrow {}^{75}\text{As}$ donor, and $^{76}\text{Ge} + \text{n} \rightarrow {}^{77}\text{Ge} \rightarrow {}^{77}\text{As} \rightarrow {}^{77}\text{Se}$ double donor. The isotopic abundance in $^{\text{nat}}$Ge and the thermal neutron capture cross sections yield a p type Ge crystal after NTD with the fixed compensation ratio K:[38]

$$K \equiv \frac{[\text{Minority Impurity}]}{[\text{Majority Impurity}]} = \frac{[\text{As}] + 2[\text{Se}]}{[\text{Ga}]} \approx 0.32 \quad (4)$$

It is therefore possible to finely tune the net-carrier concentration [Ga]–[As]–2[Se] with precise control of the neutron fluence n while maintaining the compensation ratio constant at 0.32. One of advantages of working with NTD $^{\text{nat}}$Ge is that we can reliably use other group's data recorded with NTD $^{\text{nat}}$Ge because the compensation ratio is always fixed at 0.32 and dopants are homogeneously distributed regardless of who prepares it. For the work discussed here we have prepared five samples of NTD $^{\text{nat}}$Ge. Their temperature dependence of the conductivity has been analyzed together with data reported for eight NTD $^{\text{nat}}$Ge samples by Zabrodskii and Andreev.[39]

2.2 Measurements

The electrical conductivity (σ) of the nominally uncompensated samples has been measured using a standard lock-in method at 21.0 Hz down to $T \approx 20\,\text{mK}$. The cryostat and all the analog instruments were placed inside a shielded room. The temperature of samples in a ^{3}He–^{4}He dilution refrigerator has been calibrated very carefully as described in ref. 18. Magnetic fields were applied in the direction perpendicular to the current flow by means of a superconducting solenoid. The influence of the magnetic field on the temperature calibration has been examined.[40]

The conductivity measurements of the compensated samples were performed using a ^{3}He refrigerator down to $T \approx 300\,\text{mK}$. The two point measurements with the implanted contacts were employed for many of the high resistivity samples. Sample heating was avoided by using an electrical power of less than $10^{-14}\,\text{W}$.

3. Results I: Nominally Uncompensated NTD ^{70}Ge:Ga Samples

3.1 Zero-temperature scaling analysis of the metallic samples

The temperature dependence of the electrical conductivity $\sigma(T)$ for eight samples with positive $\text{d}\sigma/\text{d}T$ in the scale of $T^{1/3}$ is shown in Fig. 1.[19] $N_{\text{c}} = 1.859 \times 10^{17}\,\text{cm}^{-3}$ for this nominally uncompensated series of samples as it will be shown later by numerical fitting with eq. (2). Based on this finding, the concentrations N of Ga of the eight samples lie between $0.994 N_{\text{c}}$ and $1.028 N_{\text{c}}$ with the top three samples being metallic at $T = 0\,\text{K}$. Mott's minimum metallic con-
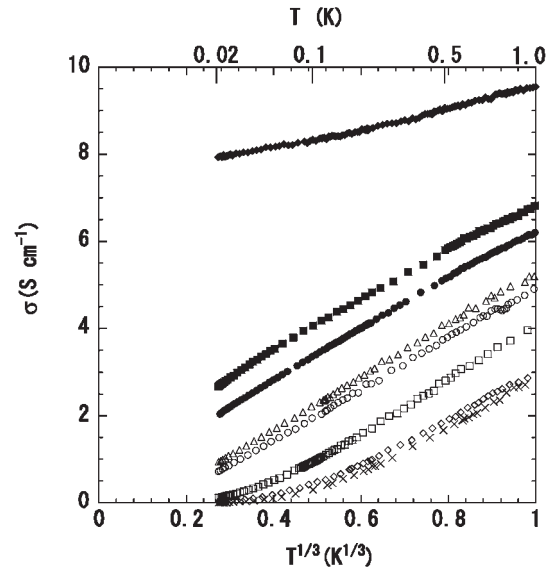

Fig. 1. Electrical conductivity vs. $T^{1/3}$ for the eight NTD ^{70}Ge:Ga samples in the vicinity of N_{c}. From bottom to top in units of $10^{17}\,\text{cm}^{-3}$, the concentrations N are 1.848, 1.850, 1.853, 1.856, 1.858, 1.861, 1.863, and 1.912, respectively. Samples with filled marks (top three curves) turn out to be metallic while the ones with other marks are insulating for $T = 0\,\text{K}$.

ductivity $\sigma_{\min}$ for Ge:Ga is estimated to be 7 S/cm using the relation $\sigma_{\min} \equiv C_{\text{M}}(e^2/\hbar)N_{\text{c}}^{1/3}$ with $C_{\text{M}} = 1/20$. The temperature dependence of $\sigma(T)$ is expected to be proportional to $T^{1/2}$ when it is governed mainly by electron–electron interaction. Therefore, $\sigma(0)$ is obtained usually by extrapolation assuming $\sigma(T) \propto T^{1/2}$, and such an analysis was performed in our earlier work.[17] However, we have subsequently found that the samples near the transition ($<1\%$ of N_{c}) obeyed $\sigma \propto T^{1/3}$ instead of $T^{1/2}$ as shown in Fig. 1.[18] This observation of the change in the temperature dependence from $T^{1/2}$ to $T^{1/3}$ as N approaches N_{c} is interesting because $T^{1/2}$ is predicted when interaction is important (Mott transition) while $T^{1/3}$ is expected[41] when disorder is dominant (Anderson transition).[42] It indicates that the nature of the transition for the two concentration regions, $N_{\text{c}} < N < 1.01 N_{\text{c}}$ and $1.01 N_{\text{c}} < N$, is different for our nominally uncompensated samples.

In ref. 18 we have developed a method that allows for an appropriate extrapolation of $\sigma(T)$ to $T = 0$ when the temperature dependence changes from $T^{1/2}$ to $T^{1/3}$ as $N \rightarrow N_{\text{c}}$. Figure 2 shows the zero-temperature conductivity $\sigma(0)$ determined for a total of twelve metallic samples, including the three metallic samples with filled marks in Fig. 1, that we measured previously[18,19] as a function of $N/N_{\text{c}} - 1$. The best fit to the twelve data points with eq. (1) yields $\mu = 0.50 \pm 0.04$ with $N_{\text{c}} = 1.860 \times 10^{17}\,\text{cm}^{-3}$,[18] i.e., $N_{\text{c}} = 1.860 \times 10^{17}\,\text{cm}^{-3}$ is employed for the horizontal axis of Fig. 2(a). On the other hand, as we will show later, the best fit with eq. (2) with a limited number of the samples within $\pm 1\%$ of N_{c} is obtained with $\mu = 1.2$ and $N_{\text{c}} = 1.859 \times 10^{17}\,\text{cm}^{-3}$, i.e., $N_{\text{c}} = 1.859 \times 10^{17}\,\text{cm}^{-3}$ is used for Fig. 2(b). Only the two metallic samples closest to N_{c} in Fig. 2(b) lie within 1% of N_{c} and they are the samples which exibit $\sigma \propto T^{1/3}$. All the samples with $N/N_{\text{c}} - 1 > 10^{-2}$ exhibit $\sigma \propto T^{1/2}$. The dashed curve is the best fit for them with $\sigma(0) \propto (N/N_{\text{c}} - 1)^{\mu}$ with $\mu = 1.2$. What is interesting is the
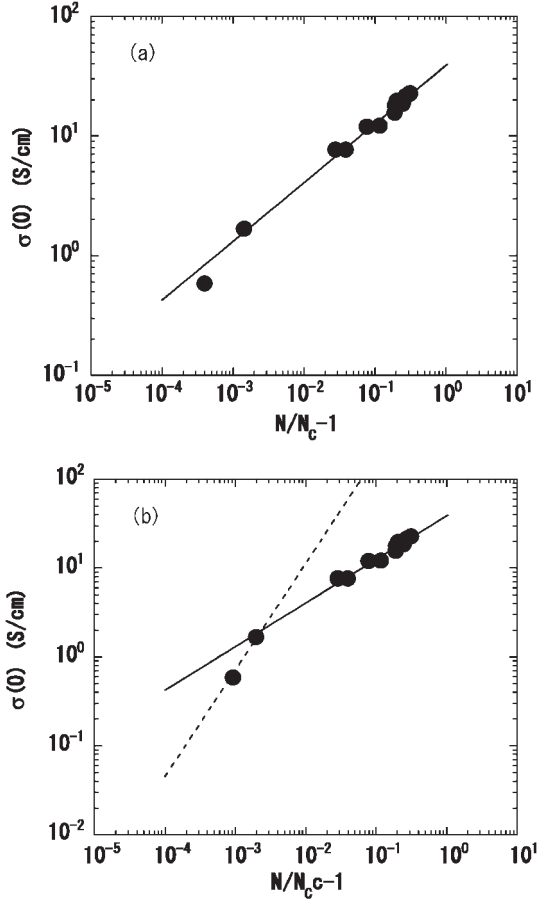
Fig. 2. Zero-temperature conductivity $\sigma(0)$ vs $N/N_c - 1$ determined experimentally ($\bullet$) by extrapolation of $\sigma(T)$ to $T = 0$ for (a) $N_c = 1.860 \times 10^{17}$ cm^{-3} and (b) $N_c = 1.859 \times 10^{17}$ cm^{-3}. They include $\sigma(0)$ for a total of twelve samples as a summary of the previous measurements.[18,19] The solid line in (a) represents the best power-law fit by $\sigma(0) \propto (N/N_c - 1)^\mu$ where $N_c = 1.860 \times 10^{17}$ cm^{-3} and $\mu = 0.50 \pm 0.04$. The dotted line in (b) is a fit for the two samples closest to N_c with $\mu = 1.2$ for it will be shown in Fig. 3(b) that the two samples obey $\mu = 1.2$ with $N_c = 1.859 \times 10^{17}$ cm^{-3} rather than $\mu = 0.5$ with $N_c = 1.860 \times 10^{17}$ cm^{-3}. The solid curve in (b) is the best fit assuming $\mu = 0.5$.

fact that there is a clear kink in $\sigma(0)$ vs $N/N_c - 1$ for the case of Fig. 2(b), and the fact that $\mu = 1.2$ applies only for the two samples that show $T^{1/3}$ dependence.

3.2 Finite temperature analysis[19]

The dependence $\sigma(N, T) \propto T^{1/3}$ at $N \sim N_c$ immediately implies $x \sim 1/3$ in eq. (2) since the contribution to the temperature dependence from the $f(|N/N_c - 1|/T^y)$ term becomes small for the region $N \sim N_c$. It was also shown in Fig. 2(a) for a wide range of the concentration $N_c < N < 1.4N_c$ that $\mu = 0.5$ when the conventional zero temperature analysis was performed with $N_c = 1.860 \times 10^{17}$ cm^{-3}. Therefore, $x = 1/3$ and $y = 2/3$ in eq. (2) are expected from the relation $\mu = x/y$ for the analysis of the wide concentration region $N_c < N < 1.4N_c$. Figure 3(a) shows the finite temperature scaling plot of $\sigma(N, T)$ using eq. (2) with $x = 1/3$, $y = 2/3$, and $N_c = 1.860 \times 10^{17}$ cm^{-3}. $\sigma(N, T)$ recorded between $T = 20$ and 750 mK was used for the analysis in Fig. 3(a). Fairly good scaling was obtained on the metallic side as expected, while scaling on the insulating side is clearly unsatisfactory. In order to find a better set of x,
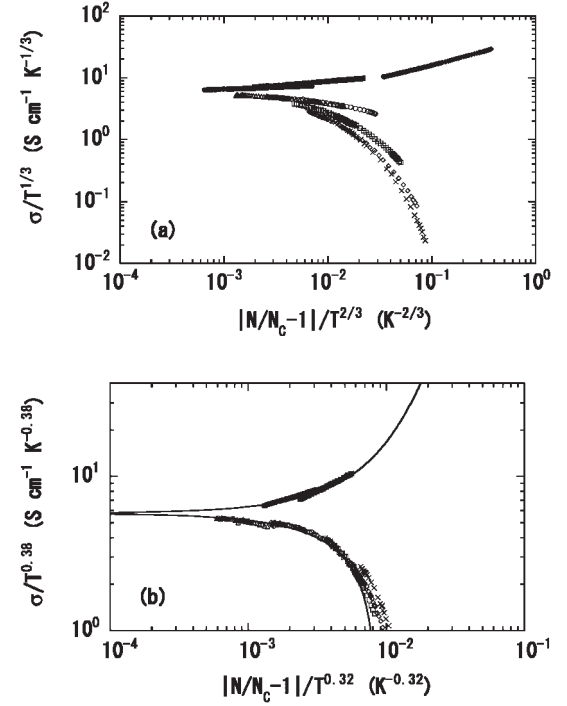

Fig. 3. Finite-temperature scaling analysis of $\sigma(N, T)$ using eq. (2) with $x = 1/3$, $y = 2/3$, and $N_c = 1.860 \times 10^{17}$ cm^{-3}, and (b) $x = 0.38$, $y = 0.32$, and $N_c = 1.8590 \times 10^{17}$ cm^{-3}. The solid curve in (b) is the best fit to the data. The symbol for each sample is the same as the one in Fig. 1.

y, and N_c, numerical fitting has been performed using the following non-linear equation;

$$\sigma(t, T) = T^x \left[a_0 + a_1 \frac{(N/N_c - 1)}{T^y} + a_2 \left(\frac{(N/N_c - 1)}{T^y} \right)^2 \right.$$
$$\left. + a_3 \left(\frac{(N/N_c - 1)}{T^y} \right)^3 \right]. \quad (5)$$

It is important to stress here that the conductivity of both the metallic and insulating samples must be described by a single scaling function, *e.g.*, eq. (5) with a single set of parameters. When we impose this strict restriction, it is not possible to achieve satisfactory fitting with eq. (5) for the samples with the wide range of N used in Fig. 3(a).

Figure 3(b) shows the result of the fitting analysis when the critical region was limited to $N = N_c \pm 0.01N_c$, i.e., only the data from five insulating and two metallic samples closest to the transition are fitted. The solid curve in Fig. 3(b) is the best fit obtained numerically with $x = 0.38$, $y = 0.32$, $N_c = 1.8590 \times 10^{17}$ cm^{-3}, $a_0 = 5.75$, $a_1 = 580$, $a_2 = 1.97 \times 10^4$, and $a_3 = 3.15 \times 10^6$ in eq. (5), which agree very well with the conductivity of both the metallic and insulating samples. A similar fit with a fourth-order equation leads to practically the same set of parameters with the absolute value of the fourth-order term being much smaller than those of the lower-order terms, i.e., third-order fitting is sufficient. The major consequence of this analysis is $\mu = x/y = 1.2 \pm 0.2$ which satisfies the Chayes *et al.*'s inequality $\mu = \nu \geq 2/3$.[26] Although the range of N we chose for scaling may appear to be quite small, we emphasize again that this range is the only region that can be scaled with eq. (2) and that the seven samples included are the only ones having $\sigma(N, T) \propto T^{1/3}$ with approximately the same slope

$d\sigma/dT^{1/3}$ (see Fig. 1).

Following the success of scaling for the very narrow $|N - N_c| \leq 0.01N_c$ region, we have attempted to scale those samples outside of the $N = N_c \pm 0.01N_c$ region, i.e., the $N \geq 0.01N_c$ and $N \leq 0.99N_c$ regions with eq. (5). The metallic side of this region is characterized by $\mu \approx 0.5$ as we have found in Fig. 2. However, even with exclusion of the $|N - N_c| \leq 0.01N_c$ samples, we could not obtain satisfactory fitting with eq. (5). Therefore, the so called $\mu \approx 0.5$ region is not scalable with the finite temperature scaling eq. (2).

3.3 Scaling of the variable range hopping resistivity as $N \to N_c$ from the insulating side[20,21]

Since it has become clear from the finite temperature scaling and the zero-temperature scaling of the metallic conductivity that the nature of the conduction within $\pm 1\%$ of N_c is different from that of outside ($N < 0.99N_c$ and $1.01N_c < N$), it becomes important to evaluate the behavior of the charge transport on the insulating side in detail.

Figure 4 shows the temperature dependence of the resistivity ρ of eighteen insulating samples in the temperature range $T = 20$–250 mK. In general the temperature dependence of the resistivity ρ for variable range hopping conduction is given by

$$\rho = \rho_0 T^q \exp(T_0/T)^p \qquad (6)$$

where $p = 1/4$ and $1/2$ have been predicted for hopping across[1] and within[43] a parabolic-shaped Coulomb gap in the density of the states, respectively. $q = 0$ is usually assumed since the temperature dependence in the strongly localized regime is determined mainly by the value of p in the exponential term. Note that $\ln \rho$ is plotted against $T^{-1/2}$ in Fig. 4 because most of the curves in the low temperature limit appear to form straight lines supporting the relation $\ln \rho \propto T^{-1/2}$. However, a closer inspection of the samples close to N_c has revealed that $q = -1/3$.[20,21] Figure 5(a) shows $\ln \rho$ vs $T^{-1/2}$ for the four samples close to N_c that do not actually obey eq. (6) when $q = 0$ is assumed. On the
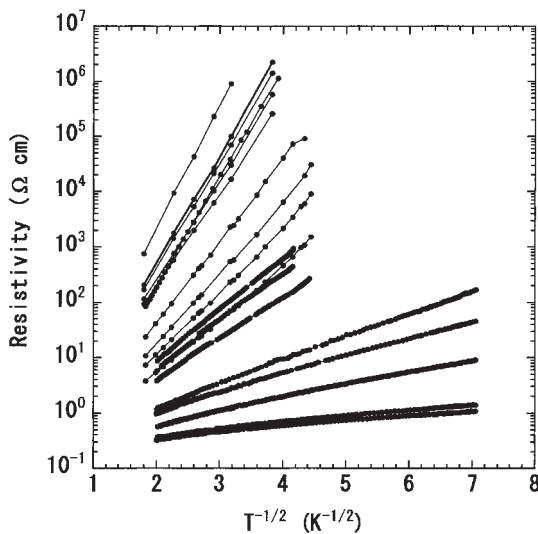
Fig. 4. $\ln \rho$ vs $T^{-1/2}$ for 18 insulating samples. The concentration N from top to bottom in the unit of N_c are 0.923, 0.943, 0.948, 0.951, 0.952, 0.957, 0.966, 0.971, 0.981, 0.986, 0.989, 0.990, 0.991, 0.992, 0.994, 0.995, 0.997, and 0.999. ($N_c = 1.859 \times 10^{17}\,\text{cm}^{-3}$).
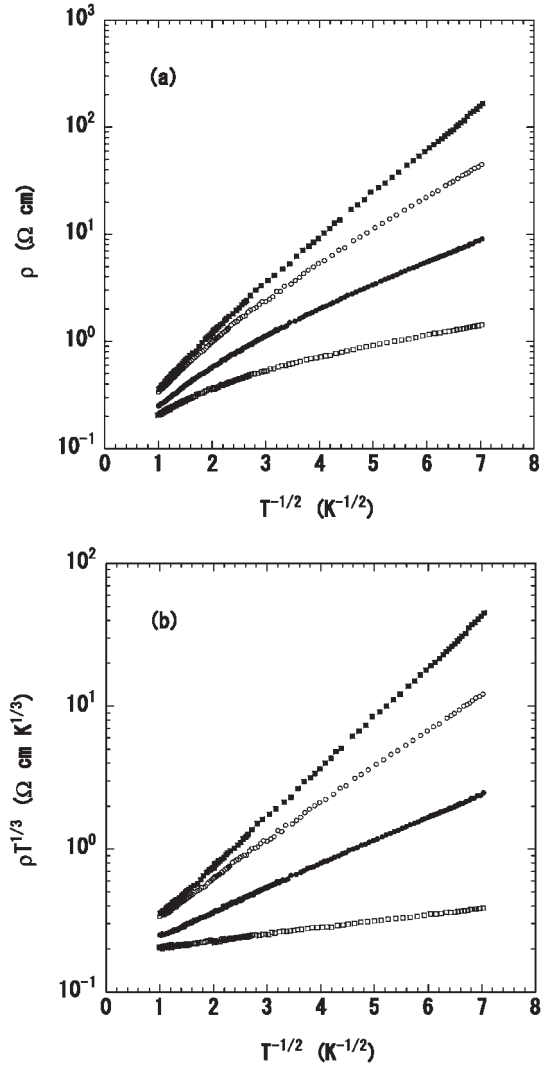
Fig. 5. (a) $\ln \rho$ vs $T^{-1/2}$ and (b) $\ln(\rho$ multiplied by $T^{1/3})$ vs $T^{-1/2}$. From top to bottom $N/N_c = 0.994, 0.995, 0.997,$ and 0.999.

other hand, it becomes consistent with eq. (6) when $q = -1/3$ is assumed as seen from the straightness of the data in the plot of $\ln \rho T^{1/3}$ vs $T^{-1/2}$ in Fig. 5(b) with respect to that in (a). $\rho \propto T^{-1/3}$ is consistent with the observation $\sigma = \rho^{-1} \propto T^{1/3}$ in Fig. 1.

Because the variable range hopping theory of Efros and Shklovskii[43] applies to our nominally uncompensated samples all the way to N_c from the insulating side, we shall use the following relation to scale T_0 in eq. (6) with $p = 1/2$ and $q = -1/3$:

$$k_B T_0 \approx \frac{1}{4\pi\epsilon_0} \frac{2.8e^2}{\epsilon(N)\xi(N)} \qquad (7)$$

in SI units, where $\epsilon(N) = \epsilon_h + \chi_{imp}(N)$ is the dielectric constant and $\xi(N)$ is the localization length. $\chi_{imp}(N)$ is the impurity dielectric susceptability and $\epsilon_h = 15.4$ is the relative dielectric constant of the host germanium. As N approaches N_c from the insulating side one expects $\chi_{imp}(N) = \chi_0(1 - N/N_c)^{-\zeta}$ and $\xi(N) = \xi_0(1 - N/N_c)^{-\nu}$. With these relations T_0 becomes

$$k_B T_0 = \frac{2.8e^2}{4\pi\epsilon_0\chi_0\xi_0}(1 - N/N_c)^\alpha, \qquad (8)$$
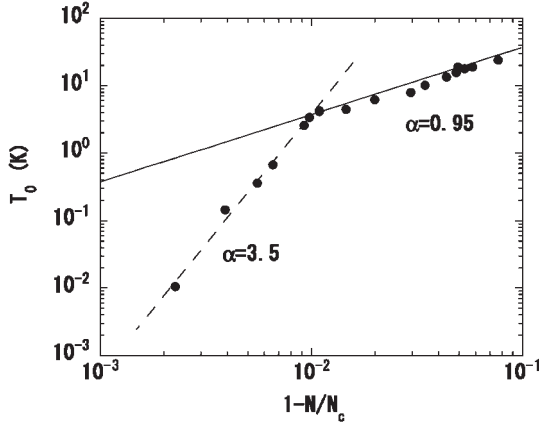
Fig. 6. T_0 as a function of $1 - N/N_c$ determined with $p = 1/2$ and $q = -1/3$ in eq. (6). The solid and dashed curves are the best fits to the data for the regions $1 - N/N_c > 10^{-2}$ and $1 - N/N_c < 10^{-2}$, respectively.

Fig. 7. Localization length ξ vs $1 - N/N_c$ (lower data set) and the dielectric susceptibility χ_{imp} arising from the impurities vs $N_c/N - 1$ (upper data set). Dashed curves are the fits to the data with $\xi(N) \propto (1 - N/N_c)^{-\nu}$ and $\chi_{imp}(N) \propto (N_c/N - 1)^{-\zeta}$.

assuming $\chi_{imp}(N) \gg \epsilon_h$ in the critical regime. The critical exponent $\alpha = \zeta + \nu$ for T_0 has been determined experimentally for our nominally uncompensated samples by evaluating the slope T_0 of each sample shown in Fig. 4 as a function of N. As seen in Fig. 6, there is a kink at 1% below N_c which divides the regions into $\alpha = 0.95 \pm 0.08$ for $0.9N_c < N < 0.99N_c$ and $\alpha = 3.5 \pm 0.8$ for $0.99N_c < N < 0.999N_c$. The solid curve in Fig. 6 represents calculated T_0 for the $0.9N_c < N < 0.99N_c$ region using eq. (8) with $\alpha = 1$, $\chi_0 = 15.4$ (dielectric constant of host Ge), and $\xi_0 = 8$ nm (Bohr radius of Ga acceptors) as was done by Ionov *et al.*,[44] which agrees surprisingly well with the data in the $\alpha = 1$ region. However, it is obvious that we expect χ_0 to be the dielectric susceptibility of a single Ga acceptor instead of $\epsilon_h = 15.4$ for the critical region. The dashed curve in Fig. 6 is the best fit to T_0 for the $0.99N_c < N < 0.999N_c$ region using eq. (8) with $\alpha = 3.5$, $\chi_0 = 2 \times 10^{-4}$, and $\xi_0 = 8$ nm. Note that the value $\chi_0 = 2 \times 10^{-4}$ is reasonable for a single Ga acceptor.

3.4 Scaling of the localization length ξ and the impurity dielectric susceptability χ_{imp} for $N \to N_c$ from the insulating side[21]

Our next step is to separate T_0 into ξ and χ_{imp} based on the magnetoresistance measurement performed on our nominally uncompensated series of insulating samples that demonstrates Efros and Shklovskii's variable range hopping conduction all the way up to N_c. For $\xi/\lambda \ll 1$, the magnetoresistance of the variable range hopping is expressed by;[43]

$$\ln[\rho(B, T)/\rho(0, T)] \approx 0.0015 (\xi/\lambda)^4 (T_0/T)^{3/2}, \quad (9)$$

where $\lambda \equiv \sqrt{\hbar/eB}$ is the magnetic length in SI units. According to eq. (9), the magnetic-field variation of $\ln \rho$ at $T = $ const. is proportional to B^2, i.e., $\ln \rho(B, T) = \ln \rho(0, T) + C(T)B^2$, and the slope $C(T)$ is proportional to $T^{-3/2}$. Since eq. (9) is equivalent to

$$\gamma \equiv C(T)/T^{-3/2} \approx 0.0015(e/\hbar)^2\xi^4 T_0^{3/2}, \quad (10)$$

ξ is given by

$$\xi \approx 5.1(\hbar/e)^{1/2}\gamma^{1/4}T_0^{-3/8}. \quad (11)$$

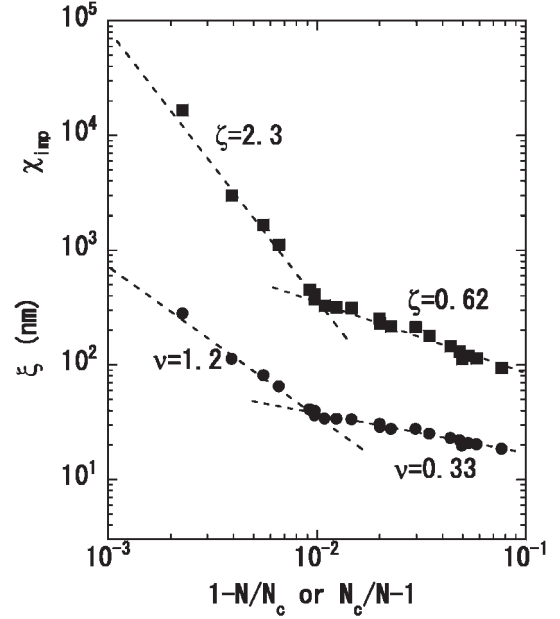Therefore, it is possible to determine ξ of each sample from the magnetoresistance measurements and calculate χ_{imp} using eqs. (7) and (11). Details of such procedures have been given in ref. 21.

Figure 7 shows ξ and $\chi_{imp} = \epsilon - \epsilon_h$ determined for our nominally uncompensated samples.[21] We should note that both ξ and χ_{imp} are sufficiently larger than the Bohr radius (8 nm for Ge) and static host dielectric constant of Ge ($\epsilon_h = 15.4$), respectively. Just like for the case of T_0 shown in Fig. 6, both ξ and χ_{imp} show sharp kinks at $N \approx 0.99N_c$. The concentration dependence of ξ and χ_{imp} below and above $0.99N_c$ can be independently fitted very well with the scaling formula $\xi(N) \propto (1 - N/N_c)^{-\nu}$ and $\chi_{imp}(N) \propto (N_c/N - 1)^{-\zeta}$, respectively, as shown in Fig. 7.

The most important outcome here is the experimental confirmation of Wegner's scaling law[27] $\mu \approx \nu$ (≈ 1.2) and the prediction of the scaling theory $2\nu \approx \zeta$ (≈ 2.3) for the region $0.99N_c < N < 0.999N_c$. On the other hand, $\mu \approx 0.5$ determined from the zero temperature extrapolation, is not equal to $\nu \approx 0.33$ for the region $N < 0.99N_c$, though the relation $2\nu \approx \zeta$ (≈ 0.62) is satisfied. It was already indicated by the finite temperature scaling that only the region within 1% of N_c is scalable with eq. (2). The fact that Wegner's scaling law is valid only within 1% of N_c supports our earlier finding that the scaling theory is applicable only to the region within 1% of N_c and not to the region outside for the case of the nominally compensated Ge.

Figure 8 summarizes the behavior of T_0 and $\sigma(0)$ as a function of normalized concentration N/N_c for the nominally uncompensated samples. The solid curves are the scaling curves with $\alpha = 0.95$ for the insulating samples, and $\mu = 0.5$ for the metallic samples that are valid for the samples outside of $\pm 1\%$ of N_c. The dashed curves are the scaling curves with $\alpha = 3.5$ for the insulating samples, and $\mu = 1.2$ for the metallic samples that are for inside of $\pm 1\%$ of N_c. The plot shows convincingly that the nature of the region within $\pm 1\%$ of N_c is different from that of outside.
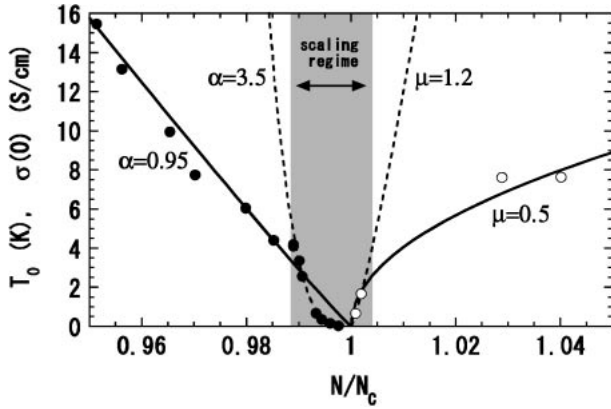
Fig. 8. T_0 (●) and $\sigma(0)$ (○) as a function of normalized cocentration N/N_c for the nominally uncompensated samples. The solid curves are the scaling curves with $\alpha = 0.95$ for the insulating samples, and $\mu = 0.5$ for the metallic samples that are outside of $\pm 1\%$ of N_c. The dashed curves are the scaling curves with $\alpha = 3.5$ for the insulating samples, and $\mu = 1.2$ for the metallic samples that are inside of $\pm 1\%$ of N_c.
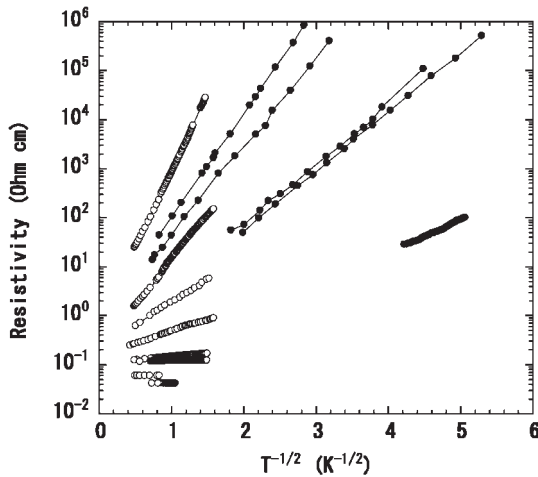
Fig. 9. $\ln \rho$ vs $T^{-1/2}$ of thirteen NTD ^{nat}Ge:Ga,As with $K = 0.32$ evaluated in this study. Filled circles represent the samples prepared and measured by the present authors while open circles are the data provided by Professor Zabrodskii.[39] The concentrations N from top to bottom in the unit of N_c are 0.25, 0.35, 0.45, 0.53, 0.56, 0.60, 0.71, 0.72, 0.93, 1.28, 1.36, 1.94, and 2.40.

4. Results II: Deliberately Compensated NTD ^{nat}Ge:Ga Samples

Figure 9 shows the temperature dependence of the resistivity for thirteen deliberately compensated ($K = 0.32$) NTD ^{nat}Ge:Ga,As samples analyzed in this study. Some of the data (open circles), which have been published in ref. 39, were provided by Professor Zabrodskii. The ranges of temperatures used for the measurements are $T = 0.25$–1 K and 0.65–2 K for filled and open circles in Fig. 9, respectively.

For our deliberately compensated series, the critical exponent $\alpha = \zeta + \nu$ for T_0 has been determined experimentally by evaluating the slope T_0 of each sample shown in Fig. 9. Similarly, the conductivity exponent μ has been determined based on the extrapolation of $\sigma(N, T)$ to $T = 0$ K. The results are summarized in Fig. 10. The least-square fitting (solid curves in Fig. 10) for the wide range of
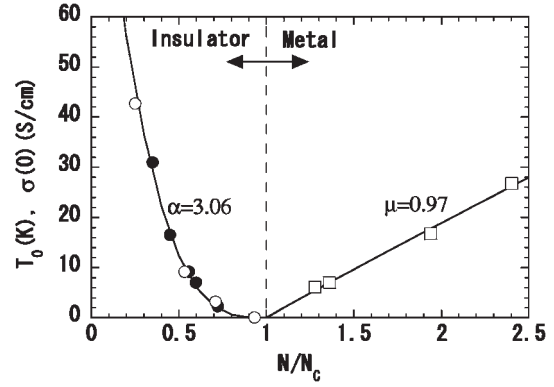

Fig. 10. T_0 (● and ○) and $\sigma(0)$ (□) as a function of normalized concentration N/N_c for the deliberately compensated, $K = 0.32$ samples. The solid scaling curves are the best fits obtained with $\alpha = 3.06$ and $\mu = 0.97$. Filled circles represent the samples prepared and measured by the present authors while open circles and squares represent the samples prepared and measured by Professor Zabrodskii and co-workers.[39]

concentration $0.25N_c < N < 2.4N_c$ yields $\alpha = 3.06 \pm 0.25$ and $\mu = 0.97 \pm 0.07$, and they are found to satisfy the expected relation $\alpha \approx 3\nu \approx 3\mu$ so that Wegner's relation $\nu = \mu$. Our results, $\alpha = 3.06 \pm 0.25$, is in excellent agreement with Rentzsch et al.'s results, $\alpha \approx 3$, previously reported for two series of n-type NTD ^{74}Ge:As with $K = 0.38$ and 0.54 in the concentration range $0.2 < N/N_c < 0.91$.[45] It was also shown by Katsumoto et al. that $\zeta \approx 2$ for compensated samples,[34] i.e., the combination of our results for deliberately compensated samples $\alpha = \nu + \zeta \approx 3$ with Katsumoto's $\zeta \approx 2$ yields $\nu \approx 1 \approx \mu$ that satisfies Wegner's scaling law. The significance of $\alpha = 3.06 \pm 0.25$ and $\mu = 0.97 \pm 0.07$ for a wide range $0.25N_c < N < 2.4N_c$ of the $K = 0.32$ series is the fact that they agree very well with $\alpha = 3.5 \pm 0.8$ and $\mu = 1.2 \pm 0.2$ for a very narrow range $0.99N_c < N < 1.01N_c$ of the nominally uncompensated series.

Figure 11 shows the finite temperature scaling of the $K = 0.32$ series. For this purpose we have performed a least-square fitting with open circles only because the open circles cover a wide range of concentrations spanning both the insulating and the metallic phases, while filled circles cover
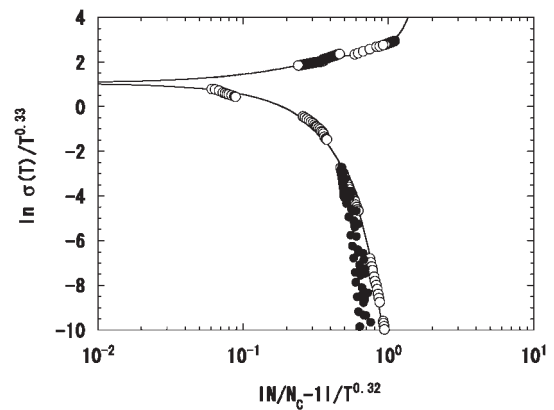

Fig. 11. Finite temperature scaling analysis of $\sigma(N, T)$ using eq. (12) with $x = 0.33$ and $y = 0.32$. The solid curve is the best fit to the data represented by open circles. Open and filled circles are the same as in Fig. 9. One in every three data points is shown for open circles.

only the limited regions of the insulating phase.

$$\ln \frac{\sigma(t,T)}{T^x} = \left[a_0 + a_1 \frac{(N/N_c - 1)}{T^y} + a_2 \left(\frac{(N/N_c - 1)}{T^y} \right)^2 \right.$$
$$\left. + a_3 \left(\frac{(N/N_c - 1)}{T^y} \right)^3 \right]. \tag{12}$$

The solid curve in Fig. 11 is the best fit obtained numerically with $x = 0.33$, $y = 0.32$, $a_0 = 1.05$, $a_1 = 4.55$, $a_2 = -5.69$, and $a_3 = 2.90$ using eq. (12). It is shown convincingly that the conductivity of the $K = 0.32$ series (especially open circles for they are the data used for fitting) collapse to form one universal curve for a very wide range of concentration $0.25 N_c < N < 2.4 N_c$. As expected, the value of the conductivity critical exponent $\mu = x/y = 1.01 \pm 0.04$ found from this analysis is in excellent agreement with $\mu = 0.97 \pm 0.07$ determined by the zero-temperature extrapolation in Fig. 10. The deviation of open and filled circles in Fig. 11 at lower temperatures is due to the fact that the data recorded in the present study (●) extend to much lower temperatures. The open circles are expected to merge with filled circles when the measurements are extended to lower temperatures. However, one sees in Fig. 11 that each series (○ and ●) collapses onto a separate single curve and the difference between the two is very small. The result of the analysis with eq. (12) is practically unchanged even if we include both open and filled circles.

5. Results III: Effect of Magnetic Field

Similar to the effect of compensation, $\mu \approx 1$ has been found experimentally for magnetic flux density B of the order of one tesla for nominally uncompensated semiconductors: Ge:Sb,[16,46] Ge:Ga,[18] Si:B,[47,48] and Si:P.[49] In order to discuss the effect of externally applied magnetic field on the nature of the MI transition, it is important to consider the length scale known as the magnetic length $\lambda \equiv \sqrt{\hbar/eB}$.[50] When a variety of length scales such as the correlation length, thermal diffusion length, inelastic scattering length, spin scattering length, and spin–orbit scattering length are larger than λ, the system is considered to be in the "magnetic-field regime". The length scale of interest to us is the correlation length ξ' on the metallic side ($N > N_c$) that diverges at $N = N_c$. When the field strength is weak, the "magnetic-field regime" where we assume $\mu \approx 1$ to hold is restricted to a narrow region of the concentration around N_c. Outside this region, the system crosses over to the "zero-field regime" where $\mu = 0.5$ is found. Such behavior is depicted in Fig. 12 where $\sigma(B,0)$, the zero-temperature conductivity at constant B, is plotted as a function of $N/N_c - 1$. The shaded region in Fig. 12 is the "magnetic-field regime" where $\lambda < \xi'$, i.e., $\mu \approx 1$, while outside of the region is the "none-magnetic-field regime" where $\lambda > \xi'$, i.e., $\mu \approx 0.5$. The correlation length ξ' as a function of $N/N_c(0) - 1$ in Fig. 12 has been estimated assuming that values of the correlation length ξ' are equal to the localization length ξ given in Fig. 7 with the mirror symmetry around N_c, i.e., $\xi(1 - N/N_c) = \xi'(N/N_c - 1)$, since the exponent is the same and the amplitude ratio is usually of the order of unity. The exponent μ obtained for the "magnetic-field regime" by eq. (1) with $t \equiv N$ and $t_c \equiv N_c$ are $\mu = 1.03 \pm 0.03$ at $B = 4$ T and $\mu = 1.09 \pm 0.05$ at
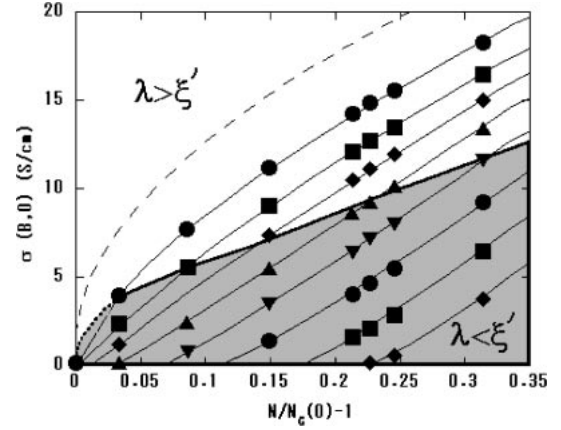

Fig. 12. Zero-temperature conductivity $\sigma(B,0)$ vs normalized concentration $N/N_c(0) - 1$, where $\sigma(B,0)$ is the zero-temperature conductivity for a constant B and $N_c(0) = 1.859 \times 10^{17}$ cm^{-3} is the critical concentration at $B = 0$. From top to bottom the magnetic flux density increases from 1 T to 8 T in steps of 1 T. The dashed curve at the top is for $B = 0$. $\mu \approx 1$ holds within the shaded region where $\lambda < \xi'$, while $\mu \approx 0.5$ is valid for outside where $\lambda > \xi'$. λ and ξ' are the magnetic and correlation lengths, respectively.
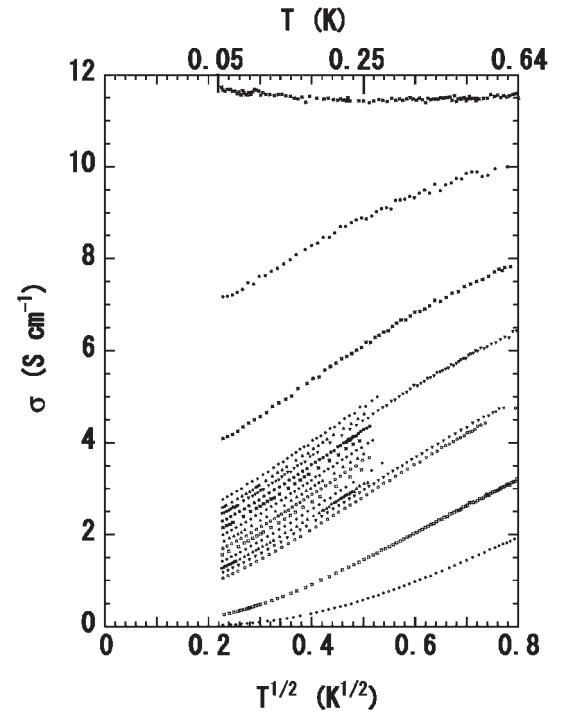

Fig. 13. $\sigma(B,T)$ vs $T^{1/2}$ of the $N = 1.063 N_c$ sample at the constant magnetic field B. From top to bottom: $B = 0, 2.0, 4.0, 4.8, 4.9, 5.0, 5.1, 5.2, 5.3, 5.4, 5.5, 5.6, 5.7, 5.8, 5.9, 6.0, 7.0$ and 8.0 T. One in every thirty data points is shown.

$B = 5$ T.

Figure 13 shows the magnetic field and temperature dependence of the conductivity $\sigma(B,T)$ of a sample having $N = 2.004 \times 10^{17}$ cm^{-3}. In contrast to Fig. 1 of the N-tuning experiment with $B = 0$, $\sigma(B,T) \propto T^{1/2}$ is observed for a wide range of constant B, i.e., $\sigma(B,T)$ is plotted against $T^{1/2}$. The zero temperature conductivity $\sigma(B,0)$ obtained by the simple extrapolation of $\sigma(B,T)$ to $T = 0$ assuming $\sigma(B,T) \propto T^{1/2}$ decreases with increasing B. This particular sample was found to undergo a MI transition at $B_c = 5.5$ T with $\mu =$
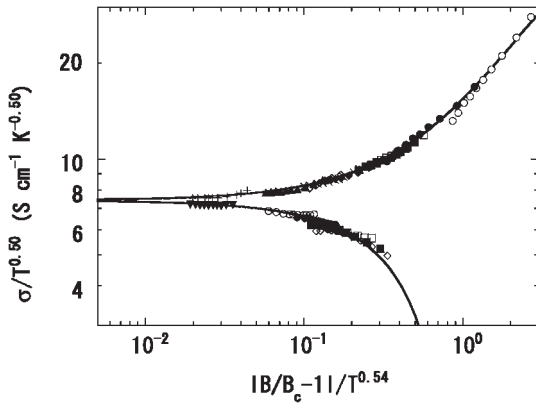
Fig. 14.   Finite temperature scaling analysis of $\sigma(B, T)$ using eq. (2) with $x = 0.50$, $y = 0.54$, and $B_c = 5.45$ T, The solid curve is the best fit to the data. The symbol for each sample is same as the one in Fig. 13.

1.1 ± 0.1 based on the analysis using eq. (1) with $t \equiv B$ and $t_c \equiv B_c$.

Figure 14 shows the finite temperature scaling of $\sigma(B, T)$ for $B = 2$–6 T and $T = 50$–500 mK for the metallic samples and $B = 2$–6 T and $T = 100$–250 mK for the insulating samples. These ranges of B and T have been chosen in order to ensure that $\sigma(B, T)$ of each sample is $\propto T^{1/2}$ with approximately the same $d\sigma/dT$ in Fig. 13. The solid curve in Fig. 14 is the best fit using eq. (2) with $t \equiv B$ and $t_c \equiv B_c$, and $x = 0.50$, $y = 0.54$, $B_c = 5.45$ T, $a_0 = 7.43$, $a_1 = 8.30$, $a_2 = -0.217$, and $a_3 = -0.063$. The conductivity critical exponent $\mu = x/y = 0.93 \pm 0.10$ obtained here for the magnetic-field tuning of a Ge:Ga with $N = 1.063 N_c$ is in good agreement with the results of the conventional extrapolation analysis $\mu = 1.1 \pm 0.1$.[22] We have shown theoretically in ref. 22 that the critical exponent μ obtained by N-tuning with constant B is equal to μ obtained by B-tuning as long as they are in the "magnetic-field regime".

6. Discussion

The critical exponents obtained for Ga:Ge are summarized in Table II. For the case of nominally uncompensated samples ($K \approx 0$) with $B = 0$, $\mu \approx 0.5$ is obtained for the wide concentration range $1.01 N_c < N < 1.4 N_c$ by the conventional extrapolation of $\sigma(T)$ to $T = 0$. However, the finite temperature scaling is not applicable to this region. $\mu \approx 0.5$ obtained from extrapolation is *not* equal to $\nu \approx 0.33$, i.e., Wegner's scaling law of $\mu = \nu$ is not satisfied, though the prediction of the scaling theory $2\nu \approx \zeta$ seems to hold for the wide range in the insulating side. It is important to notice that all of $\mu \approx 0.5$ previously reported for a variety of doped

semiconductors (see Table I) have been obtained for the wide range of concentrations on the metallic side by the extrapolation method, which means the behavior is universal. This situation changes dramatically if we limit the region to $0.99 N_c < N < 1.01 N_c$. Both the finite temperature scaling and extrapolation to zero-temperature work, and Wegner's scaling law $\mu \approx \nu \approx 1.2$ and the prediction of the scaling theory $2\nu \approx \zeta$ are satisfied. Together with $z \approx 3$, all of the critical exponents we obtain for this narrow region of nominally uncompensated Ge:Ga agree with what have been obtained with nominally uncompensated Si:P by the Karlsruhe group.[9,10] Again, this shows how universal this behavior for doped semiconductor is regardless of the material system (Si or Ge) and conduction type (n or p types). In fact, all of $\mu \approx 1$ cases listed in Table I have been found by limiting the critical region very close to N_c, as was done in our analysis.

For the case of intentionally compensated samples ($K = 0.32$) with $B = 0$, both the finite temperature scaling and extrapolation to zero-temperature work for a surprisingly large region $0.25 N_c < N < 2.4 N_c$. Wenger's scaling law $\mu \approx \nu \approx 1.0$ and the prediction of the scaling theory $2\nu \approx \zeta$ are satisfied. $z = 3$ is found from the finite temperature scaling.

For the case of nominally uncompensated samples ($K \approx 0$) with finite magnetic fields $B > 0$, the finite temperature scaling with B and T applies as long as the system is in the magnetic field regime, i.e., $\lambda < \xi'$ as shown in Figs. 12 and 14. $\mu \approx 1.0$ and $z \approx 2$ have been determined for the magnetic field induced transition.

The most distinct feature in Table II is the fact that all of the critical exponents found for $K \approx 0$ with $B = 0$ for $0.99 N_c < N < 1.01 N_c$ agree within their experimental errors with those for $K \approx 0.32$ with $B = 0$. This is a strong evidence for the fact that the critical behavior in these regions is governed by the same physics, namely doping-compensation, i.e., the width of the $\mu \approx 1$ region is determined by the degree of doping-compensation. It appear to scale with the value of K and disappear for completely uncompensated ($K = 0$) semiconductors. The experimental problem, of course, is that it is impossible to prepare $K = 0$ samples both technologically and thermodynamically.[37] The reason for the wide scattering of critical exponents μ reported for nominally uncompensated systems in Table I may be very simple; researchers have employed samples prepared in different manners (leading to different values of K) and they probed a wide variety of widths around N_c and/ or S_c, i.e., some found $\mu \geq 1$ governed by the effect of unavoidable compensation and others found $\mu \approx 0.5$ meas-

Table II.   Critical exponents of Ge:Ga. $\mu[\sigma(0)]$ have been determined by the conventional extrapolation to zero temperature using eq. (1). x and y have been determined by the finite temperature scaling [eq. (2)]. Columns with $\times$ cannot be determined because the finite temperature scaling is not applicable. Missing critical exponents (open columns) are to be determined in the future. The exponent in parentheses has been taken from ref. 34. The error bars for those not specified are typically $\sim 10\%$.

	$\mu \, [\sigma(0)]$	x	y	$\mu \, (= x/y)$	α	ν	ζ	z
$K \approx 0$, $B = 0$, $|\Delta N/N_c| > 1\%$	0.50 ± 0.04	$\times$	$\times$	$\times$	0.95 ± 0.08	0.33	0.62	$\times$
$K \approx 0$, $B = 0$, $|\Delta N/N_c| < 1\%$		0.38	0.32	1.2 ± 0.2	3.5 ± 0.8	1.2	2.3	3
$K = 0.32$, $B = 0$	0.97 ± 0.07	0.33	0.32	1.01 ± 0.04	3.06 ± 0.25	1	(≈ 2)	3
$K = 0$, $B \neq 0$	1.1 ± 0.1	0.50	0.54	0.93 ± 0.10				2

uring the region further away from N_c and S_c. A perfectly uncompensated doped semiconductor is a half-filled Hubbard system where electron–electron interaction becomes more important with respect to the effect of disorder. On the other hand, compensation introduces more positively and negatively charged ionized impurities, which act as sources of disorders. This very simple picture phenomenologically describes why the critical exponents of the "compensated region", $0.99N_c < N < 1.01N_c$ of the $K \approx 0$ series and $0.25N_c < N < 2.4N_c$ of the $K = 0.32$ series, agree with predictions of non-interacting theories. In the future it will be important to experimentally find how the width of the $\mu \approx 1$ region scale with the value of K. Growth of single crystalline Ge with controlled mixture of ^{70}Ge and ^{74}Ge followed by NTD is the ideal way to prepare samples with a controlled range of compensations.[45,51] There have been one experimental attempt to probe the critical exponents as a function of compensation. Rentzsch *et al.* have reported $\alpha \approx 1.5$ for the series with $K = 0.014$ and 0.12.[44] However, they could not resolve the two independent regions, $\alpha \approx 3.5$ for away from N_c and $\alpha \approx 1$ for near N_c because the number of samples they evaluated was limited to six. It would be of a great interest for Rentzsch *et al.* to prepare more samples, identify the two regions, and determine how the width of the "compensated region" changes as a function of the compensation.

Now we turn our attention to the effect of the magnetic field. The magnetic field, which breaks the time reversal symmetry, is expected to bring the system into a different universality class, leading to a different value of μ.[3,4] However, $\mu \approx 1$ obtained from the "compensated region" with $B = 0$ agrees with $\mu = x/y \approx 1$ obtained from the transition of the $K \approx 0$ series in the constant magnetic field (Fig. 12) and by the magnetic field (Fig. 14) within their experimental errors. One may naively conclude from this observation that the effects of the compensation and magnetic field are the same. However, one should note that the dynamical exponent $z \approx 3$ for the compensation is different from $z \approx 2$ for the magnetic field. Therefore, the universality classes of the "compensated region" and the "magnetic field region" are different.

7. Concluding Remarks

We have performed a complete scaling analysis of the low temperature electrical conductivity of nominally uncompensated and deliberately compensated Ge:Ga samples. We have determined the critical exponents for conductivity, dielectric constant, and localization and correlation lengths, and have suggested that the large scattering in the values of the critical exponents shown in Table I is due to the effect of compensation.

All aspects of the $\mu \approx \nu \approx 1$ region dominated by compensation are in complete agreement with the predictions of the original scaling theory for non-interacting system.[2] The same results have been found for nominally uncompensated Si:P and other systems, i.e., the phenomenon is universal. While everything appears to be consistent with the picture of purely disorder driven transitions, two important issues remain. The first one is the fact that more advanced calculations for purely disorder induced transitions predict $\nu = 1.57 \pm 0.02$ for the orthogonal universality class

and $\nu = 1.43 \pm 0.04$ for the unitary universality class,[52,53] while our experiment finds $\mu \approx \nu \approx 1$. Electron–electron interaction may be responsible for this small difference even though the effect of disorder is dominant for this region. The second issue relates to the question why such a wide range of concentration ($0.25N_c < N < 2.4N_c$) can be fitted with the finite temperature scaling for $K = 0.32$ while theory is expected to be valid only in the vicinity of N_c.

We believe that the $\mu \approx 0.5$ region situated outside of the $\mu \approx 1$ region is the intrinsic part of the uncompensated system. Many aspects of it do not agree with scaling theory: Wegner's scaling law is broken ($\nu \neq \mu$), the finite temperature scaling is not applicable, and $\nu \approx 0.33$ severely violates the inequality $\nu \geq 2/3$. Although there have been a number of theoretical proposals to explain these anomalous phenomena,[54–59] none of them have been accepted widely. The present experiment has revealed the anomalous aspects of the uncompensated system so unambiguously that it remains to be a theoretical challenge to describe such phenomena.

1) N. F. Mott: *Metal–Insulator Transitions* (Taylor & Francis, London, 1990) 2nd ed.
2) E. Abrahams, P. W. Anderson, D. C. Licciardello and T. V. Ramakrishnan: Phys. Rev. Lett. **42** (1979) 673.
3) P. A. Lee and T. V. Ramakrishnan: Rev. Mod. Phys. **57** (1985) 287.
4) A. Kawabata: Prog. Theor. Phys. Suppl. No. 84 (1985) 16.
5) D. Belitz and T. R. Kirkpatrick: Rev. Mod. Phys. **66** (1994) 261.
6) V. Dobrosavljevic and G. Kotliar: Phys. Rev. Lett. **78** (1997) 3943.
7) W. Sasaki: J. Phys. Soc. Jpn. **20** (1965) 825.
8) T. F. Rosenbaum, K. Andres, G. A. Thomas and R. N. Bhatt: Phys. Rev. Lett. **45** (1980) 1723.
9) S. Waffenschmidt, C. Pfleiderer and H. v. Löhneysen: Phys. Rev. Lett. **83** (1999) 3005.
10) H. Stupp, M. Hornung, M. Lakner, O. Madel and H. v. Löhneysen: Phys. Rev. Lett. **71** (1993) 2634.
11) P. F. Newman and D. F. Holocomb: Phys. Rev. B **28** (1983) 638; W. N. Shfarman, D. W. Koon and T. G. Castner: *ibid.* **40** (1989) 1216.
12) I. Shlimak, M. Kaveh, R. Ussyshkin, V. Ginodman and L. Resnick: Phys. Rev. Lett. **77** (1996) 1103.
13) P. Dai, Y. Zhang and M. P. Sarachik: Phys. Rev. Lett. **66** (1991) 1914.
14) S. Bogdanovich, M. P. Sarachik and R. N. Bhatt: Phys. Rev. Lett. **82** (1999) 137.
15) A. N. Ionov, M. J. Lea and R. Rentzsch: Pis'ma Zh. Eksp. Teor. Fiz.

54 (1991) 470 [Translation: JETP Lett. **54** (1991) 473].

16) Y. Ootuka, H. Matsuoka and S. Kobayashi: *Anderson Localization*, ed. T. Ando and H. Fukuyama (Springer-Verlag, Berlin, 1988) p. 40.

17) K. M. Itoh, E. E. Haller, J. W. Beeman, W. L. Hansen, J. Emes, L. A. Reichertz, E. Kreysa, T. Shutt, A. Cummings, W. Stockwell, B. Sadoulet, J. Muto, J. W. Farmer and V. I. Ozhogin: Phys. Rev. Lett. **77** (1996) 4058.

18) M. Watanabe, Y. Ootuka, K. M. Itoh and E. E. Haller: Phys. Rev. B **58** (1998) 9851.

19) K. M. Itoh, M. Watanabe, Y. Ootuka and E. E. Haller: Ann. Phys. (Leipzig) **8** (1999) 631.

20) K. M. Itoh: Phys. Status Solidi B **218** (2000) 211.

21) M. Watanabe, K. M. Itoh, Y. Ootuka and E. E. Haller: Phys. Rev. B **62** (2000) R2255.

22) M. Watanabe, K. M. Itoh, Y. Ootuka and E. E. Haller: Phys. Rev. B. **60** (1999) 15817.

23) M. Watanabe, K. M. Itoh, M. Morishita, Y. Ootuka and E. E. Haller: *Proc. 25th Int. Conf. Physics of Semiconductors* (Springer-Verlag, Berlin, 2001) Proceedings in Physics, Vol. 87, p. 152.

24) K. M. Itoh, M. Watanabe, Y. Ootuka and E. E. Haller: *Proc. Int. Conf. Quantum Transport and Quantum Coherence (Localization 2002)*, J. Phys. Soc. Jpn. **72** (2003) Suppl. A, p. 181.

25) E. Abrahams and G. Kotliar: Science **274** (1996) 1853.

26) J. Chayes, L. Chayes, D. S. Fisher and T. Spencer: Phys. Rev. Lett. **57** (1986) 2999.

27) F. Wegner: Z. Phys. B **25** (1976) 327.

28) T. F. Rosenbaum, G. A. Thomas and M. A. Paalanen: Phys. Rev. Lett. **72** (1994) 2121.

29) H. Stupp, M. Hornung, M. Lakner, O. Madel and H. v. Löhneysen: Phys. Rev. Lett. **72** (1994) 2122.

30) G. A. Thomas, Y. Ootuka, S. Katsumoto, S. Kobayashi and W. Sasaki: Phys. Rev. B **25** (1982) 4288.

31) M. J. Hirsch, U. Thomanschefsky and D. F. Holcomb: Phys. Rev. B **37** (1988) 8257.

32) A. G. Zabrodskii and K. N. Zinov'eva: Zh. Eksp. Teor. Fiz. **86** (1984) 727 [Translation: Sov. Phys. JETP **59** (1984) 425].

33) S. Katsumoto, F. Komori, N. Sano and S. Kobayashi: J. Phys. Soc. Jpn. **56** (1987) 2259.

34) S. Katsumoto: *Localization and Confinement of Electrons in Semiconductors*, ed. F. Kuchar, H. Heinrich and G. Bauer (Springer-Verlag, Berlin, 1990) p. 117.

35) See, for example, F. Shimura: *Semiconductor Silicon Crystal Technology* (Academic Press, San Diego, 1988) p. 159.

36) K. Itoh: Ph. D. thesis, University of California, Berkeley, 1994; Lawrence Berkeley Nat. Lab. Rep. No. 36683, 1994.

37) R. N. Bhatt and T. M. Rice: Philos. Mag. B **42** (1980) 859.

38) E. E. Haller, N. P. Palaio, M. Rodder, W. L. Hansen and E. Kreysa: *Neutron Transmutation Doping of Semiconductor Materials*, ed. R. D. Larrabee (Plenum, New York, 1984) p. 21.

39) A. G. Zabrodskii and A. G. Andreev: Pis'ma Zh. Eksp. Teor. Fiz. **58** (1993) 809 [Translation: JETP Lett. **58** (1993) 756]; A. G. Zabrodskii, A. G. Andreev and S. E. Egorov: Phys. Status Solidi B **205** (1987) 61.

40) M. Watanabe, M. Morishita and Y. Ootuka: Cryogenics **41** (2001) 143.

41) T. Ohtsuki and T. Kawarabayashi: J. Phys. Soc. Jpn. **66** (1997) 314.

42) There are other theories that explain $\sigma \propto T^{1/3}$. See for examples, B. L. Al'tshuler and A. G. Aronov: Pis'ma Zh. Eksp. Teor. Fiz. **37** (1983) 349 [Translation: JETP Lett. **37** (1983) 410] and ref. 58.

43) B. I. Shklovskii and A. L. Efros: *Electronic Properties of Doped Semiconductors* (Springer-Verlag, Berlin, 1984).

44) A. N. Ionov, I. S. Shlimak and M. N. Matveev: Solid State Commun. **47** (1983) 763.

45) R. Rentzsch, A. N. Ionov, Ch. Reich, M. Müller, B. Sandow, P. Fozooni, M. N. Lea, V. Ginodman and I. Shlimak: Phys. Status Solidi B **205** (1998) 269.

46) T. F. Rosenbaum, S. B. Field and R. N. Bhatt: Europhys. Lett. **10** (1989) 269.

47) P. Dai, Y. Zhang and M. P. Sarachik: Phys. Rev. B **45** (1992) 3984.

48) S. Bogdanovich, P. Dai, M. P. Sarachik and V. Dobrosavljevic: Phys. Rev. Lett. **74** (1995) 2543.

49) P. Dai, Y. Zhang, S. Bogdanovich and M. P. Sarachik: Phys. Rev. B **48** (1993) 4941.

50) There is an experimental evidence that the Zeeman energy may also be relavent for interacting electrons.[48] However, the magnetic length alone explains the experimental results very well in our case.

51) K. M. Itoh, W. L. Hansen, J. W. Beeman, E. E. Haller, J. W. Farmer, A. Rudnev, A. Tikhomirov and V. I. Ozhogin: Appl. Phys. Lett. **64** (1994) 2121.

52) K. Slevin and T. Ohtsuki: Phys. Rev. Lett. **78** (1997) 4083.

53) K. Slevin and T. Ohtsuki: Phys. Rev. Lett. **82** (1999) 382.

54) S. Hikami: Phys. Rev. B **24** (1981) 2671.

55) P. W. Anderson: *Localization, Interaction and Transport Phenomena*, ed. B. Kramer, G. Bergmann and Y. Bruyanseraede (Springer-Verlag, Berlin, 1985) p. 12.

56) G. S. Grest and P. A. Lee: Phys. Rev. Lett. **50** (1983) 693.

57) M. Kaveh: Philos. Mag. **52** (1985) L1; N. F. Mott and M. Kaveh: *ibid.* **55** (1987) 1; Phys. Rev. B **45** (1992) 3984.

58) J. C. Phillips: Proc. Natl. Acad. Sci. U.S.A. **94** (1997) 10528; J. Phys. Soc. Jpn. **67** (1998) 3346.

59) T. G. Castner: Phys. Rev. B **55** (1997) 4003; Phys. Rev. Lett. **84** (2000) 1539.